Effect of Thioltransferase (Glutaredoxin) Deletion on Cellular Sensitivity to Oxidative Stress and Cell Proliferation in Lens Epithelial Cells of Thioltransferase Knockout Mouse

Stefan Löfgren,[1,2,3,4] *M. Rohan Fernando,*[1,2,3] *Kui-Yi Xing,*[1,2] *Yin Wang,*[1,2] *Charles A. Kuszynski,*[5] *Ye-Shih Ho,*[6] *and Marjorie F. Lou*[1,2,7]

Purpose. To examine the physiological function of the thioltransferase (TTase)/glutathione (GSH) system in the lens using *TTase* knockout mouse ($TTase^{-/-}$) lens epithelial cells (LECs) as a model.

Methods. Primary LEC cultures were obtained from wild-type ($TTase^{+/+}$) and $TTase^{-/-}$ mice. Characterization and validation of the cells were determined by immunoblotting for TTase and α-crystallin proteins and by immunohistochemistry for glutathionylated proteins. Cell proliferation was examined by 3-(4,5-dimethyl-2-yl)-5-(3-carboxymethoxyphenyl)-2-(4-sulfophenyl)-2H-tetrazolium and BrdU analysis, and cell apoptosis after H_2O_2 stress was assessed by fluorescence-activated cell sorter analysis. Reloading of TTase protein into the $TTase^{-/-}$ cells was achieved with reagent.

Results. Primary LEC cultures obtained from wild-type ($TTase^{+/+}$) and $TTase^{-/-}$ mice were characterized and found to contain lens-specific α-crystallin protein. Western blot analysis confirmed the absence of TTase protein in the $TTase^{-/-}$ cells and its presence in the wild-type cells. $TTase^{-/-}$ LECs had significantly lower levels of glutathione (GSH) and protein thiols with extensive elevation of glutathionylated proteins, and they exhibited less resistance to oxidative stress than did $TTase^{+/+}$ cells. These cells were less viable and more apoptotic, and they had a reduced ability to remove H_2O_2 after challenge with low levels of H_2O_2. Reloading of purified TTase into the $TTase^{-/-}$ cells restored the antioxidant function in $TTase^{-/-}$ cells to a near normal state.

Conclusions. These findings confirm the importance of TTase in regulating redox homeostasis and suggest a new physiological function in controlling cell proliferation in the lens epithelial cells. (*Invest Ophthalmol Vis Sci.* 2008;49:4497–4505) DOI:10.1167/iovs.07-1404

Thioltransferase (TTase), also known as glutaredoxin, is a thiol-disulfide oxidoreductase and has cytosolic (TTase-1 or Grx1) and mitochondrial (TTase-2 or Grx2) isoforms.[1] TTase-1 is a ubiquitous heat-stable cytosolic protein with a molecular mass of 11.8 kDa.[2–4] TTase-1 receives reducing equivalents directly from glutathione (GSH) and catalyzes thiol/disulfide exchange reactions.[2,3] The active site of the enzyme contains two redox-active cysteine residues, Cys-Pro-Tyr(Phe)-Cys, and is conserved from *Escherichia coli* to mammals.[2] TTase-1 is a multifunctional enzyme involved in several important physiological processes in eukaryotic and prokaryotic cells,[5,6] including the donation of reducing equivalents to ribonucleotide reductase for DNA biosynthesis,[7] the dethiolation of protein-thiol mixed disulfides,[8,9] the regeneration of oxidatively damaged key glycolytic and oxidation defense enzymes,[8,10] the deiodination of thyroxin,[11] the reduction of oxidized ascorbate,[12,13] and the regulation of cellular signal transduction.[14]

Oxidative stress has been implicated in age-related cataract formation.[15–17] Excessive generation of reactive oxygen species (ROS) molecules from either the environment or from mitochondria of the lens epithelial cells can damage cellular macromolecules such as proteins, DNA, and lipids, leading to opacification of the lens and compromising lens transparency. Hence, lens cells are equipped with a variety of antioxidants, oxidation defense, and repair systems that can effectively remove ROS from cells and repair damaged macromolecules. Several known protein thiol oxidation damage repair systems are present in lens cells and other cells in mammals. These include the GSH-dependent TTase system for reducing protein-thiol mixed disulfides[18] and the NADPH-dependent thioredoxin/thioredoxin reductase system for reducing protein-protein disulfides.[19] Additionally, oxidized methionine in the protein can be reduced by methionine sulfoxide reductase.[20] All three systems contribute individually or synergistically to keep the lens in an overall reduced state, thus helping to maintain lens transparency.

In the present study, we investigated the cytosolic TTase/GSH system in lens cells as a protein repair system using $TTase^{-/-}$ mouse lens epithelial cells (LECs) as a model in which TTase-1 has been deleted without disrupting the mitochondrial Grx2 isoform. We studied cell integrity, cell proliferation, oxidant accumulation, and various types of oxidative damages that take place in $TTase^{-/-}$ LECs when challenged with oxidative stress conditions. Our results show that the deletion of cytosolic TTase caused a significant decrease in mouse LEC proliferation and increased sensitivity toward H_2O_2-induced oxidative stress. For simplicity, throughout this article TTase will be referred to as cytosolic TTase or TTase-1.

From the [1]Department of Veterinary and Biomedical Sciences and the [2]Center for Redox Biology, University of Nebraska-Lincoln, Lincoln, Nebraska; the [5]Departments of Pathology and Microbiology and [7]Ophthalmology, University of Nebraska Medical Center, Omaha, Nebraska; and the [6]Institute of Environmental Health Sciences, Wayne State University, Detroit, Michigan.

[3]These authors contributed equally to the work presented here and should therefore be regarded as equivalent authors.

[4]Present affiliation: St. Erik's Eye Hospital, Karolinska Institutet, Stockholm, Sweden.

Presented at the annual meeting of the Association for Research in Vision and Ophthalmology, Fort Lauderdale, Florida, April 2005.

Supported by American Heart Association Grant 0655631Z (Y-SH), National Institutes of Health Grant RO1 EY10595 (MFL), and a postdoctoral fellowship from the Swedish Medical Research Council (SL).

Submitted for publication October 30, 2007; revised April 2, 2008; accepted August 20, 2008.

Disclosure: **S. Löfgren**, None; **M.R. Fernando**, None; **K.-Y. Xing**, None; **Y. Wang**, None; **C.A. Kuszynski**, None; **Y.-S. Ho**, None; **M.F. Lou**, None

The publication costs of this article were defrayed in part by page charge payment. This article must therefore be marked "*advertisement*" in accordance with 18 U.S.C. §1734 solely to indicate this fact.

Corresponding author: Marjorie F. Lou, Department of Veterinary and Biomedical Sciences, University of Nebraska-Lincoln, 134 VBS, Lincoln, NE 68583-0905; mlou1@unl.edu.

Materials and Methods

Materials

2′, 7′-Dichlorodihydrofluorescein diacetate (DCFH-DA) was obtained from Molecular Probes (Eugene, OR). Protein transfection reagent was from Gene Therapy Systems (BioPORTER; San Diego, CA). Rabbit polyclonal antibody for αA-crystallin was purchased from Santa Cruz Biotechnology (Santa Cruz, CA). All other chemicals and reagents were standard commercial products of analytical grade.

Generation of *TTase*$^{-/-}$ Mice

DNA sequencing data showed that the mouse *TTase* gene consists of three exons. The protein coding region is located in the first two exons, whereas exon 3 contains the 3′ untranslated region of the gene. Briefly, a genomic clone containing the mouse *TTase* gene was isolated from the strain 129SV mouse genomic library. A gene-targeting vector was constructed by replacing exon 2 and some of the sequences in introns 1 and 2 with a neomycin-resistance cassette.[21] The targeting vector was linearized with *Not*I enzyme and then transfected into R1 embryonic stem cells[22] derived from (129SV × 129SVJ) F1 mice (a generous gift from Andras Nagy, Mount Sinai Hospital, Toronto, ON, Canada). Of the 298 clones screened, 51 were identified to contain the targeted *TTase* allele. One targeted clone (clone 89) was microinjected into blastocysts from C57BL/6 mice according to the standard protocol.[23] Chimeric mice derived from microinjection transmitted 129SV chromosomes into the offspring. Homozygous *TTase* knockout mice (*TTase*$^{-/-}$) were derived from breeding of heterozygous knockout mice (*TTase*$^{+/-}$) in a mixed genetic background between (129SV × 129SVJ) F1 and C57BL/6mice. Homozygous knockout mice appeared normal and healthy at 15 months of age. More details of the generation and characterization of the *TTase*$^{-/-}$ mice model will be published elsewhere.

Northern and Western Blot Analyses of Tissue from Wild-Type and *TTase* Knockout Mice

Brain, heart, and kidney tissue from wild-type (*TTase*$^{+/+}$), heterozygous *TTase* (*TTase*$^{+/-}$), and homozygous *TTase* knockout (*TTase*$^{-/-}$) mice were homogenized in guanidinium isothiocyanate solution, and total RNA was isolated according to the method described by Chirgwin et al.[24] Thirty micrograms of total RNA were denatured with glyoxal and subjected to blot analysis according to the procedures described by Thomas.[25] Eye tissue from *TTase*$^{+/+}$ and *TTase*$^{-/-}$ mice was analyzed by the same procedure for the Northern blot of TTase and G3PD (control). For protein analysis, the tissue was homogenized in 50 mM potassium phosphate buffer (pH 7.8), containing 0.1% Triton X-100, 3% glycerol, and 1 mM phenylmethylsulfonyl fluoride with a homogenizer (Polytron; Glen Mills, Clifton, NJ), followed by sonication. The homogenates were clarified by centrifugation at 20,000*g* for 15 minutes and were stored at −70°C. Protein concentrations of tissue homogenates were determined by the use of a bicinchoninic acid protein assay kit (Pierce, Rockford, IL). Thirty micrograms of tissue protein were separated on a SDS-polyacrylamide gel for protein blot analysis. The protein blot membrane was reacted with polyclonal antibodies against the whole human TTase protein generated in rabbits (Lou MF, unpublished results, 2007) and goat (American Diagnostica, Greenwich, CT).

Purification of Recombinant Human TTase

Human cDNA for TTase was cloned into pET21d (+) vector, expressed in *E. coli*, and purified using His-bind column (Novagen, Madison, WI) according to the manufacturer's protocol.

Preparation of Anti–TTase Antibody

Affinity-purified rabbit anti–TTase antibody was prepared using purified whole recombinant human TTase protein (Bethyl Laboratories, Montgomery, TX), as reported previously.[26]

Primary Mouse LEC Culture

Primary LEC cultures were prepared from four or five 2-week old wild-type (*TTase*$^{+/+}$) and *TTase*$^{-/-}$ mice in a 129SV × C57BL/6 mixed background. Mouse lens capsules with attached epithelial layers were obtained under sterile conditions and were placed in a 96-well plate containing 75 μL MEM (with 20% FBS and 50 μg/mL gentamicin)/well. This tissue was incubated for 2 to 3 weeks in a humid atmosphere with 5% CO_2 at 37°C. Medium was changed every week, and the cell plate was observed under an inverted light microscope to detect cell growth. Primary LECs that grew out of the lens capsules were subdivided and seeded at 5×10^5 cells in 60-mm tissue culture dishes.

Enzyme and Other Assays

TTase activity was assayed using a previously described method.[26] Protein concentrations in cell lysates were determined by the BCA method according to the manufacturer's protocol (Pierce Chemical, Rockford, IL), with bovine serum albumin as the standard. Lactate dehydrogenase activity was measured as described earlier.[27] GSH concentrations in cell lysates were determined using Ellman reagent.[28] Hydrogen peroxide concentration in cell culture medium was measured using the method of Hildebrant et al.[29] Glyceraldehyde-3-phosphate dehydrogenase (G3PD) activity was assayed according to the method of Bergmeyer et al.[30]

Western Blot Analysis

Proteins in cell lysates or tissue homogenates were separated by 12% SDS-PAGE and transferred to membrane (TransBlot; Bio-Rad, Hercules, CA) that was probed with anti–TTase antibodies diluted in TBST buffer (10 mM, pH 7.5, Tris-HCl, 100 mM NaCl, 0.1% Tween 20) followed by goat anti–rabbit IgG horseradish peroxidase (Santa Cruz Biotechnology). Immunodetection was performed with chemiluminescent reagent (Santa Cruz Biotechnology). The immunoblot was analyzed with an imaging system of Fluor-S MAX MultImager (Bio-Rad).

Loading of *TTase*$^{-/-}$ Mouse LECs with Purified Recombinant TTase

Purified human TTase was loaded into *TTase*$^{-/-}$ mouse LECs using a protein transfection reagent according to the manufacturer's protocol (BioPORTER; Gene Therapy Systems). This protein transfection reagent is a lipid-mediated protein delivery system that delivers protein in a functionally active form into the cytoplasm of cells. With the use of an FITC-tagged antibody (provided with the kit), the delivery efficiency of the reagent was determined by flow cytometry to be 78%. Briefly, 20 μg recombinant TTase mixed with the reagent (two BioPORTER [Gene Therapy Systems] tubes, each containing 10 μg purified recombinant TTase) was added to serum-deprived *TTase*$^{-/-}$ mouse LECs seeded in six-well plates. A control experiment was conducted using a nonrelated protein, β-galactosidase, provided with the protein transfection kit in accordance with the manufacturer's instructions. After 4 hours of incubation, the cells were washed and used for experiments.

Flow Cytometric Quantification of DCF Fluorescence in H_2O_2-Treated Wild-Type, *TTase*$^{-/-}$, and Recombinant TTase-Loaded *TTase*$^{-/-}$ Mouse Primary LECs

The membrane-permeable fluorescent dye DCFH-DA crosses the cell membrane and undergoes deacetylation by intracellular esterases, producing the nonfluorescent compound DCFH, which is trapped inside the cells. Oxidation of DCFH by ROS, including H_2O_2, produces the highly fluorescent DCF. Externally added H_2O_2 freely diffuses into the cells and oxidizes DCFH to give DCF fluorescence. Hence, DCF fluorescence intensity inside the cells is proportional to the intracellular H_2O_2 level. H_2O_2 levels in cells can be quantified by flow cytometric determination of the cellular DCF fluorescence.[31] Wild-type, *TTase*$^{-/-}$, and recombinant TTase-loaded *TTase*$^{-/-}$ mouse LECs were removed

by trypsinization, washed with Ca^{2+}- and Mg^{2+}-free phosphate-buffered saline (PBS; Sigma-Aldrich, St. Louis, MO), and resuspended in PBS containing 50 μM DCFH-DA. After 5 minutes the cells were again washed with PBS before the basal DCF fluorescence level was determined by flow cytometry (FACScan; Becton Dickinson, San Jose, CA). After a baseline was acquired, 50 μM H_2O_2 was added to all cell groups, and DCF fluorescence levels were determined at given time points. Because this 50 μM H_2O_2 did not cause oversaturation of fluorescence in the cells at the beginning of the experiment, this concentration was chosen for the flow cytometry study. Excitation was 488 nm, and green emission was measured at 525 ± 10 nm on 10,000 gated cells using log amplification. The arithmetic mean fluorescence channel was derived using flow cytometry software (CellQuest; Becton Dickinson, San Jose, CA).

Cell Proliferation and Viability Assays

Cell proliferation was determined by manual cell counting using a hemacytometer and by MTS tetrazolium reagent using assay kit (CellTiter 96 AQ_{ueous} One Solution Cell Proliferation; Promega, Madison, WI) according to the manufacturer's protocols. MTS color change was monitored (EL_X 800 Universal Microplate Reader; Bio-Tek Instruments, Winooski, VT) at 492 nm absorbance. Cell viability of wild-type and *TTase*$^{-/-}$ mouse LECs was determined after treatment with a bolus of 100 μM H_2O_2 followed by the MTS assay. Cells without H_2O_2 treatment were used as controls.

Determination of Cell Proliferation by 5-Bromodeoxyuridine Incorporation Assay

Cell proliferation of *TTase*$^{+/+}$ and *TTase*$^{-/-}$ LECs was determined with the use of a cell proliferation ELISA 5-bromodeoxyuridine (BrdU) chemiluminescence kit (Roche Applied Sciences, Indianapolis, IN). BrdU, a chemical analog of thymidine, was used in BrdU incorporation assay for cell proliferation, in accordance with the manufacturer's instructions. Briefly, cells were seeded onto black 96-well plates overnight, and medium was replaced with 2% FBS-containing MEM for another overnight. BrdU-labeling solution (final concentration, 10 μM) and PDGF (1 ng/mL) were added to serum-starved cells and incubated for 1 hour. After labeling, cells were fixed and incubated with anti–BrdU-POD. Excess antibody was removed by washing the cells with 1× PBS, and chemiluminescence was determined with a luminometer equipped with automatic substrate injectors (FLUOstar OPTIMA; BMG Labtech GmbH, Offenburg, Germany). Specific chemiluminescence was expressed as RLU/s.

Comparison of the Effect of H_2O_2 on G3PD Activity in Wild-Type, *TTase*$^{-/-}$, and Recombinant TTase-Loaded *TTase*$^{-/-}$ Mouse LECs

Wild-type, *TTase*$^{-/-}$, and recombinant TTase-loaded *TTase*$^{-/-}$ mouse LECs were gradually serum starved by incubation overnight in medium containing 1% FBS and then in serum-free medium for 30 minutes before exposure to a bolus of 150 μM H_2O_2. Cells were removed by trypsinization at 15, 30, 60, and 120 minutes, washed with PBS, and lysed with a lysis buffer. Cell lysates were centrifuged at 13,000 rpm for 10 minutes, and G3PD activity in the supernatant was determined as described.

Effect of H_2O_2 on Apoptosis in Wild-Type and *TTase*$^{-/-}$ Mouse LECs

Wild-type and *TTase*$^{-/-}$ mouse LECs at 60% to 70% confluence were incubated for 1 hour in serum-free medium with and without 50 μM H_2O_2, a concentration that did not cause severe damage to the cells, which could be recultured for apoptosis studies. Cells were then incubated for another 16 hours in medium containing 20% FBS before analysis for apoptosis. To quantify apoptosis, an Annexin V apoptosis detection kit was used (Biovision, Mountain View, CA). Annexin V detects the translocation of membrane phospholipid phosphatidylserine from the inner face of the plasma membrane to the cell surface after initiating apoptosis.[32] H_2O_2-treated cells were trypsinized and were washed once with 20% FBS-containing MEM and once with PBS. The cells were then stained with Annexin V$^-$, and 10,000 cells were analyzed by flow cytometry.

Effect of H_2O_2 on Cell Membrane Integrity

The integrity of the cell membrane was measured by following the extent of cytosolic lactate dehydrogenase (LDH) release into the medium. Wild-type and *TTase*$^{-/-}$ mouse LECs were gradually serum starved, as described, before exposure to a bolus of 150 μM H_2O_2 for 0, 15, 30, 60, and 90 minutes. The cell lysates were centrifuged, and the supernatant was analyzed for LDH activity.

Immunohistochemistry

For immunohistochemistry, cells were grown on culture slides (BD Biosciences, Bedford, MA) and fixed in freshly prepared 4% paraformaldehyde for 30 minutes. Then the cells were washed three times with PBS for 10 minutes and were blocked overnight at 4°C with 3% gelatin in PBS. Cells were covered with a monoclonal antibody (1:100 dilution) against protein-GSH mixed disulfide (Virogen, Watertown, MA) and were incubated for 2.5 hours at room temperature in a humid chamber. After this, cells were washed three times with PBS containing 0.1% Triton-X-100 for 10 minutes and were incubated with Cy5-conjugated fluorescent secondary antibodies (Molecular Probes) for 2 hours at room temperature in a dark, humid chamber. Finally, the cells were washed three times with PBS containing 0.1% Triton-X-100 and were mounted with a coverslip using anti–fade agent (MOI Biomedia, Foster City, CA). Fluorescent and phase-contrast pictures of cells were acquired with a confocal laser scanning microscope (MRC1024ES; Bio-Rad) and a 60× oil immersion objective.

Statistical Analysis

All tests were two-sided, and $P < 0.05$ was considered significant; one-way ANOVA and two-way ANOVA with replication were used to analyze the data. Subsequent to significant ANOVAs, pairwise comparisons between the *TTase*$^{+/+}$ cells and *TTase*$^{-/-}$ cells were performed by using Dunnett modified *t*-test.

Results

Northern and Western Blot Analyses of Tissue from Wild-Type and *TTase* Knockout Mice

As shown in Figure 1A, brain, heart, kidney, and eye tissue from a wild-type mouse showed a clear mRNA band for *TTase*, whereas the *TTase*$^{+/-}$ tissue had a considerably weaker mRNA band. Interestingly, a smaller *TTase* mRNA band was expressed in the *TTase*$^{-/-}$ mouse. For some reason, this smaller *TTase* was more intense in the *TTase*$^{-/-}$ eye tissue, even though G3PD control indicated that an equal amount of RNA was used in each sample (Fig. 1A). Because exon 2 of the TTase allele was deleted in the knockout mice, the mRNA expressed in the tissue of the *TTase*$^{-/-}$ mouse is likely a fused product of exon 1, with downstream sequences such as exon 3. However, Western blot analysis (Fig. 1B) of the brain, heart, and kidney tissue observed only TTase-positive bands in the tissue of wild-type and *TTase*$^{+/-}$ animals; no TTase full-sized protein was seen in tissue of *TTase*$^{-/-}$ mouse, using two sources of anti–human TTase antibody, one custom made by Bethyl Laboratories (data not shown) and another from a commercial source (American Diagnostics).

Characterization and Validation of the *TTase*$^{+/+}$ and *TTase*$^{-/-}$ Primary Mouse LECs

Primary cell cultures from *TTase*$^{+/+}$ (129SV) and *TTase*$^{-/-}$ mouse lens epithelia (in a 129SV and C57BL/6 mixed back-

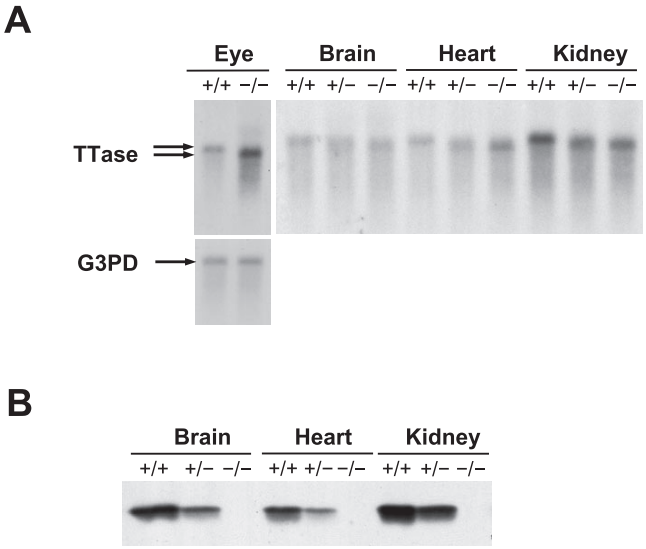

FIGURE 1. Northern and Western blot analyses of the tissue from *TTase*$^{+/+}$, *TTase*$^{+/-}$, and *TTase*$^{-/-}$ mouse. (**A**) Northern blot analysis of *TTase* mRNA expression in eye, brain, heart, and kidney tissue of wild-type and *TTase* knockout mice. The Northern blot membrane was hybridized with a full-length mouse *TTase* cDNA. G3PD mRNA analysis was used as a control for equal sample application on gel. (**B**) Western blot analysis of TTase in brain, heart, and kidney tissue of wild-type and *TTase* knockout mice. The protein blot membrane was initially reacted with rabbit anti–human TTase antibodies and then re-reacted with rabbit copper-zinc superoxide dismutase (CuZnSOD) anti–human antibodies. A duplicate protein blot membrane has also been reacted with a goat TTase-1 anti–human antiserum. (**A**, **B**) +/+, +/−, and −/− represent wild-type, heterozygous *TTase* knockout, and homozygous *TTase* knockout mice, respectively.

ground) were established and used for characterization and validation. Western blot analysis of both cell types showed the presence of the lens-specific αA-crystallin protein (Fig. 2A), confirming that the cells obtained were indeed LECs.[33] Western blot analysis also showed that TTase was present in *TTase*$^{+/+}$ cells but was not detectable in *TTase*$^{-/-}$ cells (Fig. 2B). TTase activity in *TTase*$^{-/-}$ LECs was approximately 80% less than that of *TTase*$^{+/+}$ LECs (Fig. 2C). However, loading *TTase*$^{-/-}$ LECs with human recombinant TTase using protein transfection reagent (BioPORTER; Gene Therapy Systems) resulted in increased TTase activity in *TTase*$^{-/-}$ cells (Fig. 2D). This increased TTase activity in TTase-loaded *TTase* $^{-/-}$ cells was shown to be nearly fivefold greater than in *TTase*$^{-/-}$ cells and 25% higher than normal cellular TTase activity. In contrast, TTase activity was not changed in *TTase*$^{-/-}$ cells when β-galactosidase, a non-TTase protein, was delivered by the same procedure (BioPORTER; Gene Therapy Systems; Fig. 2D).

Cell Proliferation and Morphology

Lens epithelial cells from the *TTase*$^{+/+}$ mouse were elongated, but *TTase*$^{-/-}$ cells were round and had more volume (data not shown). These cells were tightly adherent to the culture plate and were very slow in spreading, indicating impaired cell migration. Cell proliferation assessed by manual cell counting showed a significant difference ($P < 0.01$) between the *TTase*$^{+/+}$ and *TTase*$^{-/-}$ LEC cells (Fig. 3A). Deleting *TTase* had a negative effect on cell proliferation in which the approximate cell doubling time was increased from 13 hours for *TTase*$^{+/+}$ cells to 33 hours. Cell proliferation determined by the BrdU method for DNA biosynthesis also showed a significant decrease ($^{*}P < 0.05$ and $^{**}P < 0.02$) in *TTase*$^{-/-}$ cells (Fig. 3B).

Cell Viability and Membrane Integrity in the Presence of H_2O_2

Figure 4A shows a comparison of cell viability of *TTase*$^{+/+}$ and *TTase*$^{-/-}$ LECs after treatment with a bolus of 100 μM H_2O_2. Hydrogen peroxide caused an initial 50% decrease in cell viability 1 hour after treatment in both cell types, as determined by the MTS method. However, monitoring cell viability up to 6 hours after treatment showed a significant decrease ($P < 0.05$) in cell viability in *TTase*$^{-/-}$ cells compared with *TTase*$^{+/+}$ cells.

Cell membrane integrity was determined in *TTase*$^{+/+}$ and *TTase*$^{-/-}$ LECs after H_2O_2 challenge using the released LDH enzyme in the cell culture medium as an indicator. *TTase*$^{+/+}$ and *TTase*$^{-/-}$ LECs were treated with a bolus of 150 μM H_2O_2, and LDH activity in the cell culture medium was assayed at given time points (Fig. 4B). Significant LDH activity was detected in culture medium 15 minutes after the H_2O_2 challenge; thereafter, a progressive increase in LDH release was observed in *TTase*$^{+/+}$ and *TTase*$^{-/-}$ mouse LECs up to 90 minutes. However, LDH released from *TTase*$^{-/-}$ mouse LECs was much higher ($P < 0.05$) than from *TTase*$^{+/+}$ cells, indicating that the lack of TTase in cytosol affected cell membrane integrity.

GSH, Protein Thiols, and Protein-GSH Mixed Disulfides in *TTase*$^{+/+}$, *TTase*$^{-/-}$, and TTase-Loaded *TTase*$^{-/-}$ Cells

Cells that lacked TTase appeared to affect the redox status in the cells. As shown in Figure 5A, GSH content in *TTase*$^{-/-}$ cells was only 40% that of *TTase*$^{+/+}$ cells. It is well documented that oxidized GSH (GSSG) forms mixed disulfides with protein thiols; thus, protein thiol contents in *TTase*$^{+/+}$ and *TTase*$^{-/-}$ LECs were measured. As shown in Figure 5B, the protein thiol level in *TTase*$^{-/-}$ cells was only 70% that in *TTase*$^{+/+}$ cells ($P < 0.05$). Protein-GSH mixed disulfide levels in *TTase*$^{+/+}$and *TTase*$^{-/-}$ LECs were measured by immunohistochemistry with the use of mouse anti–monoclonal antibody (Virogen, Watertown, MA) and Cy5-labeled second antibody and were visualized by confocal microscopy. As shown in Figure 5C, fluorescence intensity was significantly higher in *TTase*$^{-/-}$ cells than in the *TTase*$^{+/+}$ cells, indicating that the lack of TTase resulted in an accumulation of protein-GSH mixed disulfides in the cells.

The effect of oxidative stress on the level of GSH in both cell types was compared by exposing cells to a bolus of 150 μM H_2O_2. The oxidant had no effect on GSH level in *TTase*$^{+/+}$ cells during the first 30 minutes. After that, there was a gradual decrease with less than 10% GSH loss at 90 minutes. However, the same condition caused a marked (approximately 40%) decline in GSH level in *TTase*$^{-/-}$ cells within 15 minutes. This decline continued throughout the experimental period of 90 minutes; results are summarized in Figure 5D.

H_2O_2 Detoxification in *TTase*$^{+/+}$, *TTase*$^{-/-}$, and TTase-Loaded *TTase*$^{-/-}$ Cells

ROS marker DCF fluorescence in *TTase*$^{+/+}$ and *TTase*$^{-/-}$ LECs was measured by fluorescence-activated cell sorter (FACS). H_2O_2 at 50 μM was chosen for this detoxification study because this low level did not generate fluorescence overload in the cells that would interfere with the FACS analysis. As shown in Figure 6, neither type of cell showed endogenous ROS (DCF fluorescence) at the time. After the addition of a bolus of H_2O_2 (50 μM), the DCF fluorescence gradually increased in both groups. Mean DCF fluorescence in the *TTase*$^{-/-}$ group was progressively elevated to 120 mean value within 5.5 minutes, whereas *TTase*$^{+/+}$ cells showed only 20 to 30 mean fluorescence value, which was maintained throughout the 5.5-minute

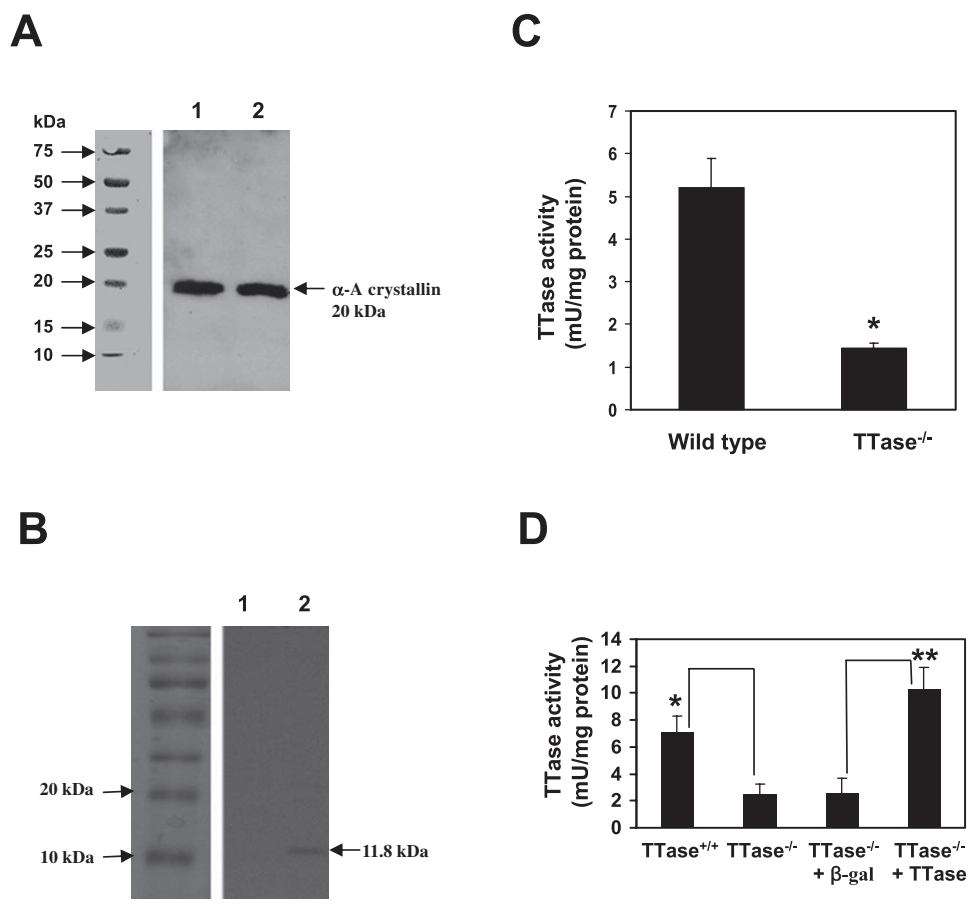

FIGURE 2. Characterization and validation of *TTase*$^{+/+}$ and *TTase*$^{-/-}$ mouse LECs. Immunoblot analysis of *TTase*$^{+/+}$ and *TTase*$^{-/-}$ mouse LECs. Mouse LEC layers were obtained from wild-type and *TTase*$^{-/-}$ mouse and homogenized. These homogenates were analyzed by SDS-PAGE and subjected to immunoblot analysis using either anti–α-A crystalline antibody or anti–human TTase antibody. (**A**) Detection of α-A crystallin in wild-type and *TTase*$^{-/-}$ LECs. (**B**) Detection of TTase in wild-type and *TTase*$^{-/-}$ LECs. *Lane 1*: *TTase*$^{-/-}$ LECs. *Lane 2*: *TTase*$^{+/+}$ LECs. (**C**) TTase enzyme activity in *TTase*$^{+/+}$ and *TTase*$^{-/-}$ LEC lysates. Error bars indicate SD. $n = 5$. *Significant difference from the *TTase*$^{+/+}$ cells ($P < 0.05$). (**D**) TTase activity in *TTase*$^{+/+}$, *TTase*$^{-/-}$, TTase-loaded *TTase*$^{-/-}$, and β-galactosidase–loaded *TTase*$^{-/-}$ mouse LECs. Human recombinant TTase (20 μg) and β-galactosidase (20 μg) were introduced into *TTase*$^{-/-}$ cells using protein transfection reagent. Error bars indicate SD, $n = 5$. *$P < 0.05$; **$P < 0.05$.

experimental period, indicating that *TTase*$^{+/+}$ LECs have an ability to detoxify H_2O_2 for cellular protection. Purified human recombinant TTase was loaded into *TTase*$^{-/-}$ LECs using the protein transfection reagent to examine whether reloading TTase into the *TTase*$^{-/-}$ LECs would restore the H_2O_2 detoxification efficiency of *TTase*$^{-/-}$ cells. As shown in Figure 2D, loading purified TTase into *TTase*$^{-/-}$ LECs successfully increased TTase activity in those cells. *TTase*$^{-/-}$ cells reloaded with purified TTase behaved similarly to *TTase*$^{+/+}$ cells and showed little difference in accumulated ROS (Fig. 6). This strongly suggested that the depletion of TTase from LECs impaired the ability of the cells to effectively detoxify H_2O_2 and probably all ROS.

Effect of H_2O_2 on Glyceraldehyde 3-Phosphate Dehydrogenase Activity in *TTase*$^{+/+}$ and *TTase*$^{-/-}$ LECs

Glyceraldehyde 3-phosphate dehydrogenase (G3PD) is easily oxidized and inactivated by forming glutathionylated G3PD; the inactivated G3PD activity can be restored by TTase.[34] Therefore, we examined the status of G3PD activity in *TTase*$^{+/+}$ and *TTase*$^{-/-}$ cells after challenge with oxidative stress. Treating both *TTase*$^{+/+}$ and *TTase*$^{-/-}$ LECs with a bolus of 150 μM H_2O_2 caused significant reduction ($P < 0.05$) in G3PD activity in both cell types (Fig. 7A), but the activity loss (30% at 30 minutes) in *TTase*$^{+/+}$ cells was gradually restored to nearly 90% after 120 minutes (Fig. 7A). However, in *TTase*$^{-/-}$ cells, the G3PD activity loss was earlier and more severe (approximately 70% loss within 15 minutes) with much less reactivation (65% of the original activity) than in *TTase*$^{+/+}$ cells (Fig. 7A). These data suggest that the depletion of TTase caused a significant decrease in the cell's ability to protect G3PD from H_2O_2-mediated inactivation. Figure 7B summarizes the percentage of remaining G3PD activity (compared with untreated control) in *TTase*$^{+/+}$ and *TTase*$^{-/-}$ cells with and without reloading of pure TTase 15 minutes after H_2O_2 treatment. The reintroduction of TTase into *TTase*$^{-/-}$ cells significantly improved the ability of these cells to protect G3PD from H_2O_2 inactivation (Fig. 7B).

Effect of H_2O_2 on Apoptosis in Wild-Type and *TTase*$^{-/-}$ Mouse LECs

Under normal growth conditions, approximately 10% *TTase*$^{+/+}$ cells underwent early stage of apoptosis, whereas cells lacking TTase showed nearly 30% apoptosis (Fig. 8), indicating that TTase may have some protective function against early-stage apoptosis. We used a 50-μM bolus of H_2O_2 to induce apoptosis in *TTase*$^{+/+}$ and *TTase*$^{-/-}$ LECs because this level of stress still allows the cells to reattach 60 minutes after treatment. Under this stress condition, there was no change in apoptosis in *TTase*$^{+/+}$ cells (Fig. 8). However, treating *TTase*$^{-/-}$ cells with a 50-μM bolus of H_2O_2 induced nearly 75% of the cells to enter an early stage of apoptosis (Fig. 8), further suggesting that TTase protects cells from H_2O_2-induced apoptosis.

DISCUSSION

The primary lens epithelial cell cultures used in this study were established from *TTase*$^{+/+}$ and *TTase*$^{-/-}$ mouse lens epithelia and were validated to contain the lens-specific αA-crystallin protein.[33] Because the tissue of *TTase*$^{-/-}$ mice, including the eye, expresses a truncated form of *TTase* mRNA from the

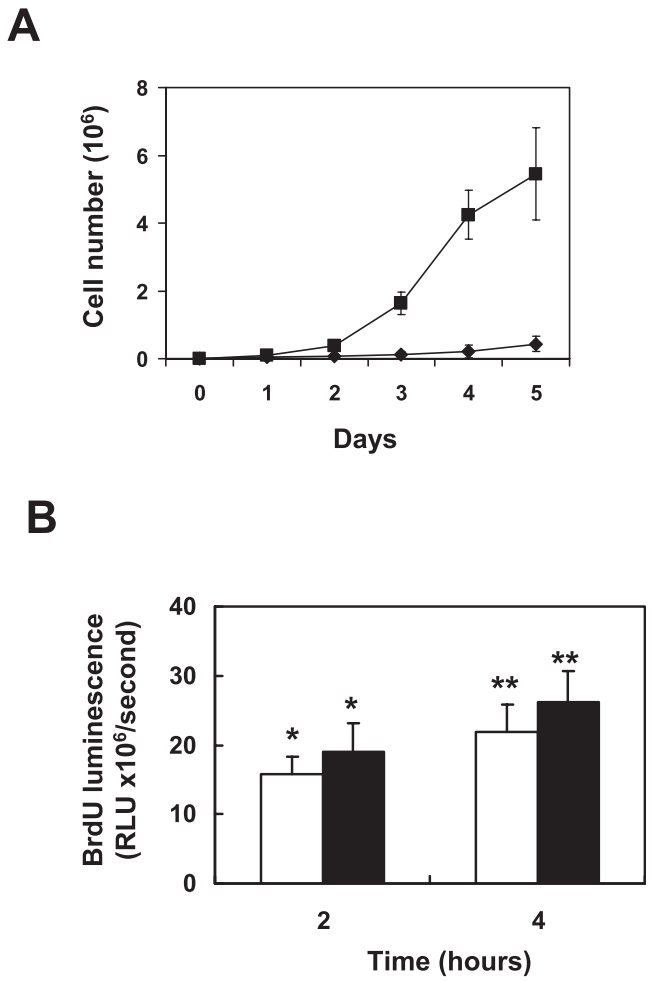

FIGURE 3. Comparison of cell proliferation of *TTase*$^{+/+}$ and *TTase*$^{-/-}$ mouse LECs in culture. (**A**) *TTase*$^{+/+}$ (■) and *TTase*$^{-/-}$ (◆) LEC proliferation determined by manual cell counting. Error bars indicate SD; $n = 5$. *$P < 0.01$. (**B**) Comparison of *TTase*$^{+/+}$ (■) and *TTase*$^{-/-}$ (□) LEC proliferation by BrdU incorporation. *$P < 0.05$; **$P < 0.02$.

fusion of exon 1 and exon 3 sequences, it is conceivable that the same *TTase* mRNA is also expressed in LECs isolated from these mice. The upregulation of truncated *TTase* mRNA in the null eye probably reflects a compensatory upregulation of gene activity in response to loss of TTase function. The mouse TTase is 107 amino acids long, and its C-terminal 38 amino acids are encoded by exon 2. The exon 1–exon 3 fusion mRNA expressed from the targeted TTase allele would allow extension of the reading frame into the noncoding region of exon 3 to include 17 more amino acids, resulting in a protein that is 21 amino acids shorter (because of the deletion of exon 2) than in the wild-type protein. The active site of TTase protein (23-Cys-Pro-Tyr-Cys-26) is encoded by exon 1. However, 13 of 14 amino acids in the GSH-binding site, which are encoded by the exon 2 sequence, would be missing in the mutant protein. This may greatly affect the structure and function of the mutant TTase protein in the knockout mice. Toward this end, we examined the expression of TTase protein in various tissue and LECs from knockout mice using two different preparations of antibodies against the human TTase (both antibodies were made against the entire length of TTase protein). These studies show that no TTase protein could be detected in tissue or LECs of homozygous knockout mice (Figs. 1B, 2B). We also could not detect any truncated TTase protein that might be expressed from the mutated *TTase* gene, suggesting that if the mutant TTase protein were produced, because of its extreme short half-life, the protein would have been degraded in the process. Even if it were not degraded, the phenomenon of oversensitivity to oxidation exhibited by the *TTase*$^{-/-}$ cells could not have been caused by the truncated TTase proteins because *TTase*$^{-/-}$ cells could be normalized when pure TTase protein was delivered into the *TTase*$^{-/-}$ cells. This strongly suggests that the abnormal property of the *TTase*$^{-/-}$ cells is caused by a lack of TTase-1, not by possible toxicity from the truncated TTase protein in the lenses of *TTase* knockout mice.

The residual TTase activity shown in the *TTase*$^{-/-}$ cells likely resulted from a mitochondrial isoform of TTase-2 (glutaredoxin 2), a recently identified member of the TTase family.[35] However, TTase-2 is too low to be seen by Western blot analysis under our current conditions. These experiments established that the primary cell cultures we used were mouse LECs and that the cells obtained from *TTase*$^{-/-}$ mouse lenses were devoid of TTase. Because wild-type mice (*TTase*$^{+/+}$) with the same genetic background as that of *TTase*$^{-/-}$ mice were used for isolation of LECs, the increased susceptibility of *TTase*$^{-/-}$ cells to oxidative stress observed in our study is believed to have resulted from the deficiency of TTase but not from the differences of the mouse genetic background.

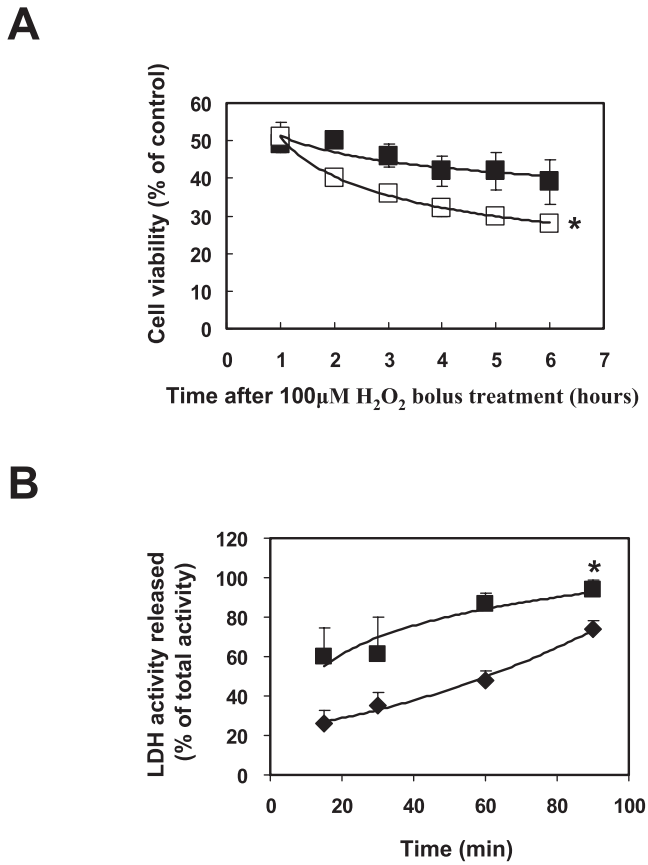

FIGURE 4. Effect of H_2O_2 on cell viability and LDH release in *TTase*$^{+/+}$ and *TTase*$^{-/-}$ LECs. (**A**) Determination of *TTase*$^{+/+}$ (■) and *TTase*$^{-/-}$ (□) LEC viability by MTS reagent. *TTase*$^{+/+}$ and *TTase*$^{-/-}$ LECs were treated with a bolus of 100 μM H_2O_2 for indicated times, and then MTS color change was measured using an ELISA plate reader at 490 nm. MTS reagent was added to the cells 1 hour before absorbance measurements. (**B**) LDH release of *TTase*$^{+/+}$ (◆) and *TTase*$^{-/-}$ (■) LECs. Cells were treated with a bolus of 150 μM H_2O_2 for the indicated times, and the cell culture medium was collected for LDH activity measurements. LDH activity was determined as described and expressed as a percentage of total LDH activity in the cells. Error bars indicate SD. $n = 5$. *Significant difference from the *TTase*$^{+/+}$ cells ($P < 0.05$).

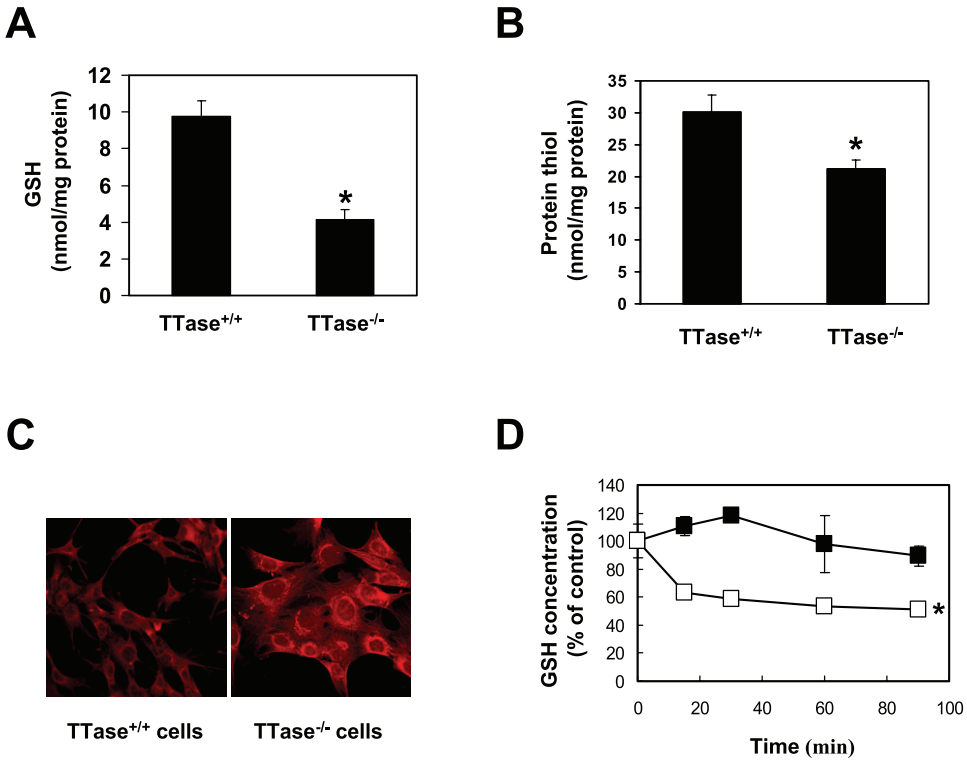

FIGURE 5. GSH, protein thiol, and protein-GSH mixed disulfide levels and effect of H_2O_2 on GSH level of *TTase*$^{+/+}$ and *TTase*$^{-/-}$ LECs. (**A**) GSH level of *TTase*$^{+/+}$ and *TTase*$^{-/-}$ LECs. (**B**) Protein thiol level of *TTase*$^{+/+}$ and *TTase*$^{-/-}$ LECs. (**C**) Comparison of protein-GSH mixed disulfide level of *TTase*$^{+/+}$ and *TTase*$^{-/-}$ LECs using immunohistochemistry. Original magnification, ×60. (**D**) Effect of a bolus of 1.5 mM H_2O_2 treatment on GSH level of *TTase*$^{+/+}$ and *TTase*$^{-/-}$ LECs. *TTase*$^{+/+}$ and *TTase*$^{-/-}$ LECs were treated with H_2O_2, and GSH concentration was determined spectrophotometrically, as described, at indicated time points and expressed as a percentage of control. Results are based on the average of five determinations. Error bars indicate SEM. *Significant difference from the *TTase*$^{+/+}$ cells ($P < 0.05$).

TTase depletion in lens epithelial cells showed a wide range of effects to the function and survival of the cells, including slower cell proliferation, decreased cell viability, and increased sensitivity to oxidative stress-induced damage. In comparison with the wild-type LECs, *TTase*$^{-/-}$ cells were rounder and tightly attached to the culture plate, and they migrated very slowly (data not shown). It has been reported that actin deglutathionylation plays a key role in growth factor–mediated actin polymerization, translocation, and reorganization near the cell periphery, which are important steps in cell migration.[36] The slow cell migration we observed in *TTase*$^{-/-}$ cells may be the result of impaired deglutathionylation of actin. As assessed by manual cell counting and BrdU incorporation, deleting *TTase* extensively lowered the rate of cell proliferation. DNA biosynthesis was low in *TTase*$^{-/-}$ cells, as measured by BrdU incorporation (Fig. 3B). It is likely that the impaired cell proliferation observed in *TTase*$^{-/-}$ cells might have been the result of decreased DNA biosynthesis, which requires TTase as a hydrogen donor for ribonucleotide reductase.[7]

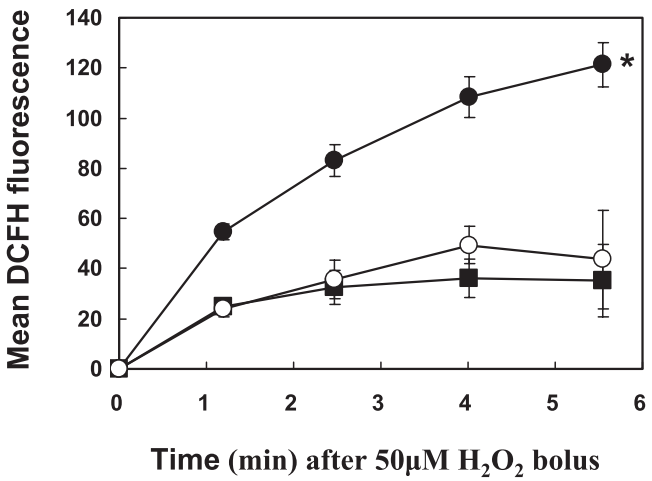

FIGURE 6. H_2O_2 detoxification in *TTase*$^{+/+}$, *TTase*$^{-/-}$, and TTase-loaded *TTase*$^{-/-}$ mouse LECs. FACS analysis of the time course of mean DCF fluorescence intensity of *TTase*$^{+/+}$ (■), TTase-loaded *TTase*$^{-/-}$ (○), and *TTase*$^{-/-}$ (●) LECs treated with 50 μM H_2O_2. Error bars indicate SD. $n = 5$. *Significant difference from the *TTase*$^{+/+}$ and TTase-loaded *TTase*$^{-/-}$ cells ($P < 0.05$).

Earlier studies carried out in our laboratory have shown that inhibiting TTase activity in HLE B3 cells by cadmium before H_2O_2 treatment caused a marked decrease in cell viability.[34] *TTase*$^{-/-}$ cells also exhibited impaired cell viability and cell membrane integrity under conditions of H_2O_2 stress (Figs. 4A, 4B), confirming the importance of TTase in maintaining cell viability and protecting the cell membrane from oxidant-induced damage. GSH and protein thiol levels were lower in *TTase*$^{-/-}$ cells than in *TTase*$^{+/+}$ cells (Figs. 5A, 5B). We hypothesized that those low levels of GSH and protein thiols resulted from the accumulation of glutathionylated proteins in *TTase*$^{-/-}$ cells because deglutathionylation requires TTase. With the use of monoclonal anti–GSH antibody, which specifically recognizes glutathionylated proteins, we showed that the glutathionylated protein level was much higher in TTase$^{-/-}$ cells than in *TTase*$^{+/+}$ cells (Fig. 5C). Furthermore, exposing both cell types to H_2O_2 stress showed a marginal GSH depletion effect only in *TTase*$^{+/+}$cells but more extensive and prolonged GSH loss in the *TTase*$^{-/-}$ cells, further indicating that protein deglutathionylation was indeed severely impaired by the absence of TTase in the cells. Progressive loss of GSH and protein thiols and the accumulation of glutathionylated proteins are the hallmark of aging and cataractous lens epithelial cells.[16] In this regard, *TTase*$^{-/-}$ cells appear to resemble the epithelial cells from aging and cataractous lenses.

Compared with *TTase*$^{+/+}$ cells, *TTase*$^{-/-}$ cells were inefficient in decomposing H_2O_2. Interestingly, loading *TTase*$^{-/-}$ cells with purified recombinant TTase resulted in normalization of the ability of these *TTase* knockout cells to decompose H_2O_2 (Fig. 6). This inefficiency might have resulted from low

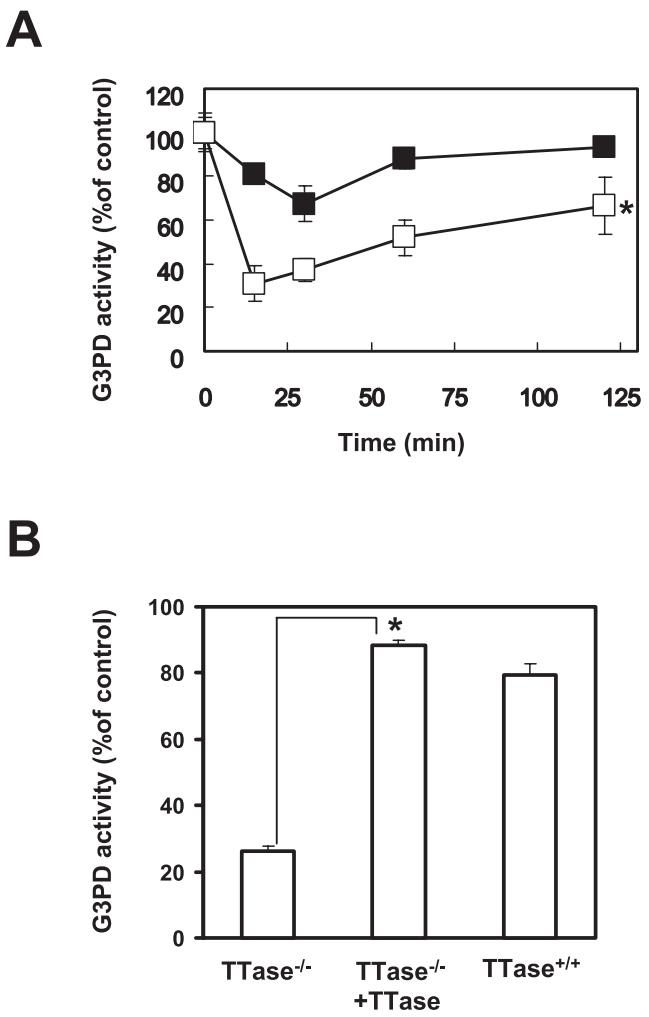

FIGURE 7. Effect of H_2O_2 on G3PD activity in *TTase*$^{+/+}$, *TTase*$^{-/-}$, and TTase-loaded *TTase*$^{-/-}$ LECs. (**A**) Comparison of G3PD activity of *TTase*$^{+/+}$ and *TTase*$^{-/-}$ LECs after oxidative stress. Cultured *TTase*$^{+/+}$ (■) and *TTase*$^{-/-}$ (□) LECs were treated with a 150-μM bolus of H_2O_2 for indicated times, and then cell lysates were prepared and G3PD activity was assayed as described. Results are based on the average of five determinations. Error bars indicate SEM. (**B**) The percentage of G3PD activity remained in the *TTase*$^{+/+}$, *TTase*$^{-/-}$, and TTase-loaded *TTase*$^{-/-}$ LECs 15 minutes after treatment with a 150-μM bolus of H_2O_2. Each cell group without H_2O_2 treatment was considered the control. Results are based on the average of 5 determinations. Error bars indicate SEM. $^*P < 0.05$.

GSH levels in *TTase*$^{-/-}$ cells given that GSH is essential for the function of glutathione peroxidase in cellular H_2O_2 detoxification. Even though TTase itself has no peroxidase activity, it has been shown to enhance the activity of certain peroxiredoxins in plant cells.[37] Therefore, the effect of TTase on cellular H_2O_2 removal, as we observed in this study, was probably contributed by a similar TTase property in mammalian cells.

Protection and regeneration of G3PD activity from H_2O_2-induced oxidative stress was also markedly reduced in *TTase*$^{-/-}$ cells compared with *TTase*$^{+/+}$cells. Loading *TTase*$^{-/-}$ cells with recombinant TTase, however, significantly improved cellular ability to protect G3PD from H_2O_2-mediated inactivation (Figs. 7A, 7B). Reactivation of oxidatively inactivated G3PD is a known function of TTase. G3PD is a key glycolytic enzyme for ATP supply in the cells with critical cysteine residues highly sensitive to oxidants such as H_2O_2. The molecular nature of the H_2O_2-mediated inactivation of purified G3PD in vitro has been shown to be the oxidation of the critical cysteine residues to monothiol-oxidation products such as sulfenic acid.[38] In many cell types, however, including the lens epithelial cells, it has been demonstrated that H_2O_2 inactivated G3PD by inducing the formation of protein-GSH mixed disulfide[34,39] and that TTase can effectively reactivate G3PD by removing the protein-GSH mixed disulfide at the active site.[34] The observation that *TTase*$^{-/-}$ cells had impaired cell viability and cell membrane integrity might have been the result of impaired H_2O_2 decomposition and protein/enzyme reactivation.

Furthermore, previously published data implicate that TTase is an antiapoptotic protein. TTase obtained from *E. coli* protected cerebellar granule neurons from dopamine-induced apoptosis by activating Ras-phosphoinositide 3-kinase and jun N-terminal kinase pathways.[40] Conversely, TTase inhibition by cadmium led to the initiation of apoptosis,[41] suggesting an important role for TTase in protecting cells against apoptosis. Our studies using *TTase*$^{-/-}$ cells confirm those previous findings and establish TTase as an important cellular enzyme that confers protection against oxidant-induced apoptosis.

Ho et al.[23] recently reported that a *TTase* knockout mouse line with deleted exons 1 to 3 did not display any extra susceptibility to acute oxidation-induced injury in heart and lung when the animal was subjected to ischemia/reperfusion or hyperoxia. Cells isolated from embryonic fibroblasts of the knockout mouse were selectively sensitive to oxidants such as diquat and paraquat but not to H_2O_2 or diamide. These contrasting results suggest that different tissue and cell types may depend differently on TTase protection. Because of the unique location of the eye, the lens in particular is more sensitive to oxidative stress and consequently is more sensitive to the loss of any redox regulating enzymes, such as TTase. Our current findings further substantiate the unique oxidative-sensitive nature of the lens tissue.

In summary our study provides strong evidence that TTase is an important enzyme in protecting LECs from oxidative damage through its involvement in reducing H_2O_2 level, regen-

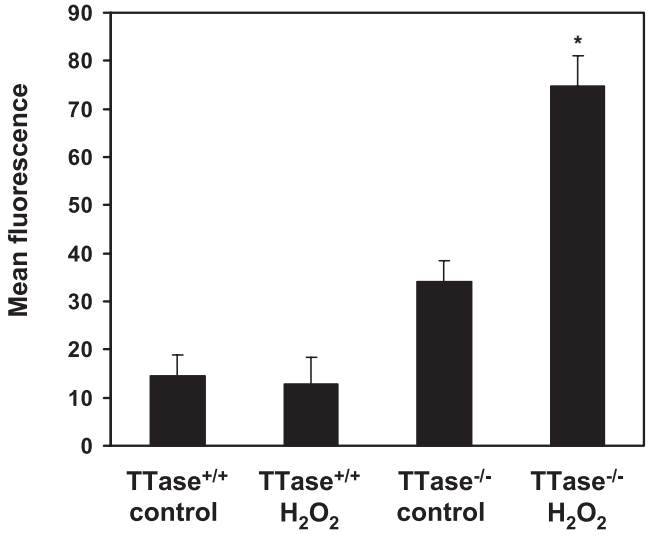

FIGURE 8. Effect of H_2O_2 on apoptosis of *TTase*$^{+/+}$ and *TTase*$^{-/-}$ LECs. *TTase*$^{+/+}$ and *TTase*$^{-/-}$ LECs were treated with 50 μM H_2O_2 in serum-free medium for 1 hour, and then medium was replaced with new MEM with 10% FBS and incubated at 37°C for 16 hours. The cells were trypsinized, washed with PBS, stained with Annexin V-FITC, and analyzed by flow cytometry. Ten thousand cells were analyzed, and the mean fluorescence channel was derived. Results are based on the average of five determinations. Error bars indicate SEM. *Significant difference from the *TTase*$^{+/+}$ control cells ($P < 0.05$).

erating oxidatively damaged proteins/enzymes, and acting as an antiapoptotic agent.

Acknowledgments

The authors thank You Zhou of the Center of Biotechnology, University of Nebraska-Lincoln, for conducting the immunohistochemical study.

References

1. Askelof P, Axelsson K, Eriksson S, Mannervik B. Mechanism of action of enzymes catalyzing thiol-disulfide interchange: thioltransferases rather than transhydrogenases. *FEBS Lett*. 1974;38:263–267.
2. Wells WW, Yang Y, Deits TL, Gan ZR. Thioltransferases. *Adv Enzymol Relat Areas Mol Biol*. 1993;66:149–201.
3. Holmgren A. Glutathione-dependent synthesis of deoxyribonucleotides: purification and characterization of glutaredoxin from *Escherichia coli*. *J Biol Chem*. 1979;254:3664–3671.
4. Fernando MR, Sumimoto H, Nanri H, et al. Cloning and sequencing of the cDNA encoding human glutaredoxin. *Biochim Biophys Acta*. 1994;1218:229–231.
5. Holmgren A. Thioredoxin and glutaredoxin systems. *J Biol Chem*. 1989;264:13963–13966.
6. Lou MF. Protein-thiol mixed disulfides and thioltransferase in the lens: a review. In: Green K, Edelhauser HF, Hackett RB, Hull DS, Potter DE, Tripathi RC, eds. *Advances in Ocular Toxicology*. New York: Plenum; 1997;27–46.
7. Holmgren A. Hydrogen donor system for *Escherichia coli* ribonucleoside-diphosphate reductase dependent upon glutathione. *Proc Natl Acad Sci U S A*. 1976;73:2275–2279.
8. Yoshitake S, Nanri H, Fernando MR, Minakami S. Possible differences in the regenerative roles played by thioltransferase and thioredoxin for oxidatively damaged proteins. *J Biochem (Tokyo)*. 1994;116:42–46.
9. Wang G-M, Raghavachari N, Lou MF. Relationship of protein-glutathione mixed disulfide and thioltransferase in H_2O_2-induced cataract in cultured pig lens. *Exp Eye Res*. 1997;64:693–700.
10. Xing KY, Lou MF. Effect of H_2O_2 on human lens epithelial cells and the possible mechanism for oxidative damage repair by thioltransferase. *Exp Eye Res*. 2002;74:113–122.
11. Goswami A, Rosenberg IN. Purification and characterization of a cytosolic protein enhancing GSH-dependent microsomal iodothyronine 5′-monodeiodination. *J Biol Chem*. 1985;260:6012–6019.
12. Wells WW, Wu DP, Yang YF, Rocque PA. Mammalian thioltransferase (Glutaredoxin) and protein disulfide isomerase have dehydroascorbate reductase activity. *J Biol Chem*. 1990;265:15361–15364.
13. Fernando MR, Satake M, Monnier V, Lou MF. Thioltransferase mediated ascorbate recycling in human lens epithelial cells. *Invest Ophthalmol Vis Sci*. 2004;45:230–237.
14. Stark DW, Chock PB, Mieyal JJ. Glutathione-thiyl radical scavenging and transferase properties of human glutaredoxin (thioltransferase)—potential role in redox signal transduction. *J Biol Chem*. 2003;278:14607–14613.
15. Lou MF. Redox regulation in the lens. *Prog Retin Eye Res*. 2003; 22:657–682.
16. Spector A. Oxidative stress-induced cataract: mechanism of action. *FASEB J*. 1995;9:1173–1182.
17. Augusteyn RC. Protein modification in cataract: possible oxidative mechanisms. In: Duncan G, ed. *Mechanisms of Cataract Formation in the Human Lens*. New York: Academic Press; 1981;72–115.
18. Raghavachari N, Lou MF. Evidence for the presence of thioltransferase in the lens. *Exp Eye Res*. 1996;63:433–441.
19. Yegorova S, Liu A, Lou MF. Human lens thioredoxin: molecular cloning, and functional characterization. *Invest Ophthalmol Vis Sci*. 2003;44:3263–3271.
20. Kantorow M, Hawse JR, Cowell TL, et al. Methionine sulfoxide reductase A is important for lens cell viability and resistance to oxidative stress. *Proc Natl Acad Sci U S A*. 2004;101:9654–9659.
21. Nagy A, Rossant J, Nagy R, Abramow-Newerly W, Roder JC. Derivation of completely cell culture-derived mice from early-passage embryonic stem cells. *Proc Natl Acad Sci U S A*. 1993;90:8424–8428.
22. Bradley A. Production and analysis of chimeric mice. In: Robertson EJ, ed. *Teratocarcinomas and Embryonic Stem Cells: A Practical Approach*. Oxford, UK: 1987;113–151.
23. Ho A, Xiong Y, Ho DS, et al. Targeted disruption of the glutaredoxin 1 gene does not sensitize adult mice to tissue injury induced by ischemia/reperfusion and hyperoxia. *Free Red Biol Med*. 2007; 43:1299–1312.
24. Chirgwin JM, Przybyla AE, MacDonald RJ, Rutter WJ. Isolation of biologically active ribonucleic acid from sources enriched in ribonuclease. *Biochemistry*. 1979;18:5294–5299.
25. Thomas PS. Hybridization of denatured RNA and small DNA fragments transferred to nitrocellulose. *Proc Natl Acad Sci U S A*. 1980;77:5201–5205.
26. Qiao F, Xing K, Liu A, Ehlers N, Raghavachari N, Lou MF. Human lens thioltransferase: cloning, purification, and function. *Invest Ophthalmol Vis Sci*. 2001;42:743–751.
27. Bergmeyer HU, Bernt E. Lactate dehydrogenase: UV-assay with pyruvate and NADH. In: Bergmeyer HU, ed. *Methods of Enzymatic Analysis*. 2nd ed. New York: Academic Press; 1974;574–579.
28. Ellman GL. A colorimetric method for determining low concentration of mercaptans. *Arch Biochem Biophys*. 1958;74:443–450.
29. Hildebrant AG, Roots I, Tjoe M, Heinemeyer G. Hydrogen peroxide in hepatic microsomes. *Methods Enzymol*. 1978;52:342–350.
30. Bergmeyer HU, Grassi M, Walter HE. Glyceraldehyde 3-phosphate dehydrogenase. In: Bergmeyer HU, ed. *Methods of Enzymatic Analysis*. 3rd ed. Weinheim: Verlag Chemie; 1983:210–211.
31. Bass DA, Parce JW, Dechatelet LR, Szejda P, Seeds MC, Thomas M. Flow cytometric studies of oxidative product formation by neutrophils: a graded response to membrane stimulation. *J Immunol*. 1983;130:1910–1917.
32. Fadok VA, Voelker DR, Campbell PA, Cohen JJ, Bratton DL, Henson PM. Exposure of phosphatidylserine on the surface of apoptotic lymphocytes triggers specific recognition and removal by macrophages. *J Immunol*. 1992;148:2207–2216.
33. Wang X, Garcia CM, Shui Y-B, Beebe DC. Expression and regulation of α-, β-, and γ-crystallins in mammalian lens epithelial cells. *Invest Ophthalmol Vis Sci.* 2004;45:3608–3619.
34. Xing K, Lou MF. The possible physiological function of thioltransferase in cells. *FASEB J*. 2003;17:2088–2090.
35. Gladyshev VN, Liu A, Novoselov SV, et al. Identification and characterization of a new mammalian glutaredoxin (thioltransferase), Grx2. *J Biol Chem.* 2001;276:30374–30380.
36. Wang J, Tekle E, Oubrahim H, Mieyal JJ, Stadtman ER, Chock PB. Stable and controllable RNA interference: investigating the physiological function of glutathionylated actin. *Proc Natl Acad Sci U S A*. 2003;100:5103–5106.
37. Matsuda NH, Motohashi K, Yoshimura H, et al. Anti-oxidative stress systems in cyanobacteria: significance of type II peroxiredoxin and the role of 1-cys peroxiredoxin in synechocytis sp. strain PCC 6803. *J Biol Chem*. 2004;280:840–846.
38. Little C, O'Brien PJ. Mechanism of peroxide-inactivation of the sulphyldryl enzyme glyceraldehydes-3-phosphate dehydrogenase. *Eur J Biochem*. 1969;10:533–538.
39. Grant CM, Quinn KA, Dawes IW. Differential protein S-thiolation of glyceraldehydes-3-phosphate dehydrogenase isoenzymes influences sensitivity to oxidative stress. *Mol Cell Biol*. 1999;19:2650–2656.
40. Daily D, Vlamis-Gardikas A, Offen D, et al. Glutaredoxin protects cerebellar granule neurons from dopamine-induced apoptosis by dual activation of the Ras-phosphoinositide 3-kinase and jun N-terminal kinase pathways. *J Biol Chem*. 2001;276:21618–21626.
41. Chrestensen CA, Starke DW, Mieyal JJ. Acute cadmium exposure inactivates thioltransferase (Glutaredoxin), inhibits intracellular reduction of protein glutathionyl-mixed disulfide, and initiates apoptosis. *J Biol Chem*. 2000;275:26556–26565.